

# Cubic Phase in a Connected Micellar Network of Poly(propylene oxide)–Poly(ethylene oxide)–Poly(propylene oxide) Triblock Copolymers in Water

Kell Mortensen

Department of Solid State Physics, Risø National Laboratory, DK-4000 Roskilde, Denmark

Received March 25, 1996; Revised Manuscript Received August 22, 1996<sup>®</sup>

**ABSTRACT:** Small-angle neutron scattering studies are presented in the solid aqueous gel phase of the Pluronic-R polymer, 25R8, which is a triblock copolymer with a central poly(ethylene oxide) block symmetrically surrounded by poly(propylene oxide) blocks:  $\text{PO}_{15}\text{EO}_{156}\text{PO}_{15}$ . At copolymer concentrations of the order of 50–65 w/w %, these copolymers associate into a homogeneous phase constituting an interconnected network of micelles, in which micellar cores of hydrophobic poly(propylene oxide) are interconnected by hydrophilic poly(ethylene oxide) strands. At temperatures below 40 °C, the materials form three solid gel phases. Neutron scattering shows that two of these phases have characteristics of cubic structures. The third phase constitutes a mixture of ordered micelles and a lamellar phase of crystalline PEO. The cubic phase close to the order-to-disorder transition can by shear be aligned into a mono (or twin) domain structure, resulting in a novel polymer network in which the knots are positioned on a lattice.

## I. Introduction

Block copolymer surfactants presently attract great interest both as a result of their commercial utility and because of their novel physical behavior. Many studies have been performed on aqueous solutions of triblock copolymers of poly(ethylene oxide) (PEO) and poly(propylene oxide) (PPO) as recently reviewed.<sup>1–4</sup>

It is well established that aqueous solutions of PEO–PPO–PEO in wide temperature/concentration ranges associate into spherical micellar aggregates along with rodlike and possibly layered micelles.<sup>5–8</sup> The spherical micelles constitute the basis for *gel* formation in the form of a body-centered cubic (BCC) mesophase.<sup>4,6,7</sup> Coming from low temperature/low polymer concentrations, the formation of this cubic mesophase is understood as a simple hard-sphere crystallization, since changing either temperature or polymer concentration leads to a linear increase in micellar volume fraction.<sup>6</sup> At the high temperature/high polymer concentration boundaries, the cubic phase dissociates as a result of changes in the micellar form.

Aqueous suspensions of the reversed block copolymer architecture, PPO–PEO–PPO, show rather different phase behavior. But also this system is dominated by spherical micelles in a wide region of the phase diagram.<sup>9</sup> Due to the hydrophobic blocks situated at both ends, however, the block copolymer associates into a *network of micelles* rather than the independent micelles in PEO–PPO–PEO systems.

In the present paper, we will show that it is possible to form an ordered phase of such micellar networks; i.e., one can make a polymer network in which the knots are distributed on a lattice, which in the present case is cubic.

## II. Experimental Section

**A. Material.** The triblock copolymer, poly(propylene oxide)–poly(ethylene oxide)–poly(propylene oxide),  $[\text{OCH}_2\text{CH}(\text{CH}_3)]_{15}\text{H}[\text{OCH}_2\text{CH}_2]_{156}[\text{OCH}_2\text{CH}(\text{CH}_3)]_{15}$  or  $\text{PO}_{15}\text{EO}_{156}\text{PO}_{15}$  (or PPO–PEO–PPO), abbreviated 25R8, was obtained from BASF Corp. (Wyandotte, MI). The molecular weight of the copolymer

given by the manufacturer is  $M_{25R8} = 8550$ , corresponding to  $M_{\text{PEO}} = 6840$  and  $M_{\text{PPO}} = 2 \times 855$ . The triblock copolymer was used without further purification.

The block copolymer was mixed with water ( $\text{D}_2\text{O}$ ) at ambient temperature and then heated to roughly 60 °C to make a homogeneous sample. The samples were sealed and stored at high temperatures for more than 24 h in order to reach equilibrium. Deuterium oxide ( $\text{D}_2\text{O}$ ) was used in order to achieve good contrast and low background in the neutron scattering experiments.

**B. Small-Angle Neutron Scattering.** Small-angle neutron scattering experiments were performed using the Risø SANS facility. Most of the experiments were performed with the samples mounted in a sealed Couette shear cell.<sup>10</sup> A few additional studies were made in a parallel-plate shear device, which is a Rheometrics Solid Analyzer II modified to be used *in situ* in the neutron beam.

The results presented below were obtained using neutrons with 6 Å wavelength, with a sample-to-detector distance of 3 m, giving scattering vectors in the range  $0.01\text{--}0.1\text{ Å}^{-1}$ , where the scattering vector  $\vec{q}$  is given by the scattering angle  $\theta$  and the neutron wavelength  $\lambda$ :  $|\vec{q}| = q = (4\pi/\lambda) \sin(\theta/2)$ . The neutron wavelength resolution was  $\Delta\lambda/\lambda = 0.18$ , and the neutron beam collimation was determined by pinholes of 16 and 7 mm diameter at the source and sample positions, respectively, and the collimation length was equal to the sample-to-detector distance. The smearing induced by the wavelength spread, the collimation, and the detector resolution were included in the data analysis discussed below, using Gaussian approximations for the different terms. The scattering data were corrected for the background arising from the shear cell with  $\text{D}_2\text{O}$  and from other sources, as measured with the neutron beam blocked by plastic containing boron at the sample position. The incoherent scattering from  $\text{H}_2\text{O}$  was used to determine deviations from a uniform detector response.

The scattering data were all, within the resolution, reproducible in terms of heating and cooling cycles. Within the measuring protocol reported below, we did not observe any time dependence.

**C. Rheology.** Viscoelastic measurements have already been reported in ref 9. Below, we have included and redrawn those rheological measurements which are relevant for the present paper. These studies were performed using a temperature-controlled Bohlin VOR rheometer, with a 0.15 Hz frequency and a strain amplitude less than 0.004. The samples were placed in the Couette cell as a liquid at high temperature. Storage and loss moduli,  $G'$  and  $G''$ , were measured as a function of temperature. The heating and cooling rates were  $\pm 0.25\text{ °C/min}$ .

<sup>®</sup> Abstract published in *Advance ACS Abstracts*, January 1, 1997.

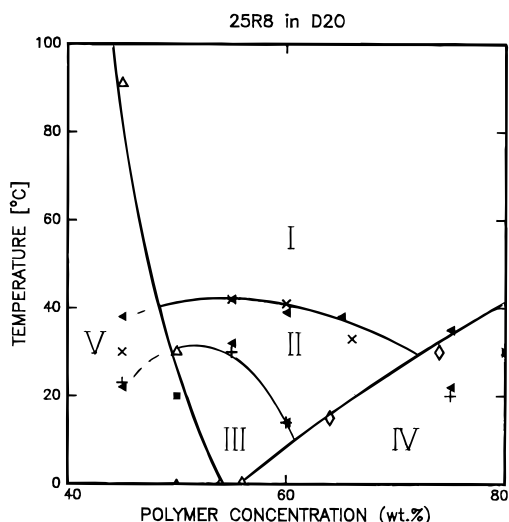


**Figure 1.** Temperature-concentration phase diagram of 25R8 in the 40–80% polymer concentration range. Phases I and V are disordered micellar networks, V with excess water. Phases II and III are cubic micellar phases. Phase IV is a coexistence regime of micelles and crystalline layered PEO.

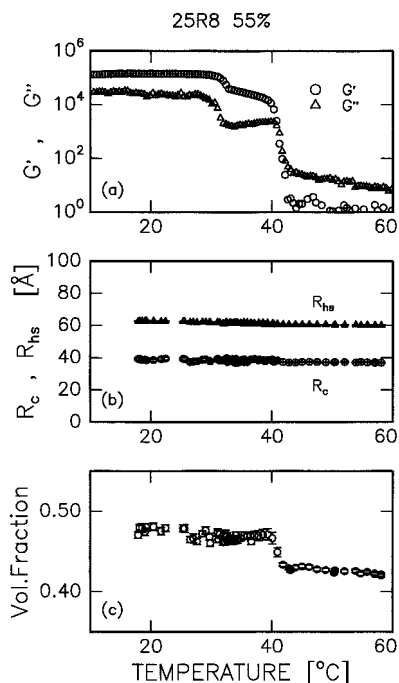


**Figure 2.** (a) Elastic modulus  $G'$  from oscillatory shear measurements of a 55% 25R8 suspension. (b) Micellar core radius and micellar hard-sphere interaction radius, and (c) micellar volume fraction, as obtained from Percus–Yevick fits to the scattering functions.

### III. Results and Discussion

Figure 1 shows the part of the phase diagram that is relevant for the present study. The phase diagram is obtained from the combined rheological and structural data reported previously<sup>9</sup> and the data presented below. In order to facilitate subsequent referral, we have given the various phases numbers from I to V: I and V are liquid-like micellar network phases, I being homogeneous and V having excess water. The II–IV phases are all solid-like gels.

**A. Rheology.** Figure 2a shows the shear modulus of a 55% 25R8 suspension, as reproduced from ref 9. At high temperatures the sample shows a small elastic modulus, and the loss modulus is larger than the elastic

term,  $G'' > G'$ . Over a narrow interval of temperatures close to  $T_c = 42^\circ\text{C}$ ,  $G'$  shows a strong increase by 4–5 orders of magnitude.  $G'$  now exceeds  $G''$ , marking a transition to a solid phase. The rheological properties at the  $T_c = 42^\circ\text{C}$  transition is reversible with respect to both transition temperature and elastic moduli.<sup>9</sup>

At  $T_s = 30^\circ\text{C}$  a second transition appears where the shear modulus increases by an additional order of magnitude. This transition from a softer to a more rigid solid-like phase seems somewhat less reproducible with regard to elastic parameters; however, the same transition temperature is found in both the oscillatory equipment used for rheology studies and the continuous shear in the SANS Couette cell, indicating that the rheologically observed transition is not an artifact due to changes in the dynamical regime.

Qualitatively similar behavior is observed for samples between roughly 50 and 70% concentrations.<sup>9</sup> The most rigid solid-like structure is observed for concentrations near 55%, and the softer structures appear at both higher and lower concentrations.

**B. Structure.** Structural analysis using small-angle neutron and light scattering methods have revealed that the aqueous solutions of 25R8 within the range 50–70%, as discussed in the present paper, is dominated by micelles interconnected into a network through the association of the two end blocks into different micellar cores.<sup>9</sup> The dominant feature of the scattering function of 25R8 as measured by neutrons is a correlation peak. While the peak intensity for polymer concentrations below approximately 35% increases with increasing temperature, the higher concentration materials shows the reverse behavior.<sup>9</sup>

Within the regime of 50–70% polymer, the scattering function can effectively be analyzed in terms of simple hard-sphere interacting micelles, using the Percus–Yevick approximation.<sup>8–11</sup> The scattering function can then be written

$$I(q) = \Delta\rho^2 N F_s(q) S(q) \quad (1)$$

where  $F_s(q)$  to a good approximation is determined by the core of the micelle and is approached by the form factor of a dense sphere with radius  $R_c$ :

$$F_s(q) = \left[ \frac{3}{(qR_c)^3} (\sin(qR_c) - qR_c \cos(qR_c)) \right]^2 \quad (2)$$

and the structure factor  $S(q)$  given by the hard-sphere interaction radius  $R_{hs}$  and volume fraction  $\phi$ ,

$$S(q) = \frac{1}{1 + 24\phi G(2qR_{hs}, \phi)/(2qR_{hs})} \quad (3)$$

$G$  being a trigonometric function of  $R_{hs}$  and  $\phi$ .  $\Delta\rho$  is the scattering contrast between the micellar core and the liquid phase and  $N$  is the number of micelles. Representative fits to the data are shown in Figure 3.

The resulting hard-sphere interaction distance, as shown in Figure 2b varies only slightly with temperature, decreasing from  $R_{hs} = 62 \text{ \AA}$  at  $10^\circ\text{C}$  to  $R_{hs} = 60 \text{ \AA}$  at  $60^\circ\text{C}$ . The core radius shows correspondingly only minor temperature dependence, namely  $R_c = 39 \text{ \AA}$  at  $10^\circ\text{C}$  and  $R_c = 37 \text{ \AA}$  at  $60^\circ\text{C}$ . Within experimental statistics, there is no observable change in micellar dimensions at any of the two transition temperatures observed rheologically.

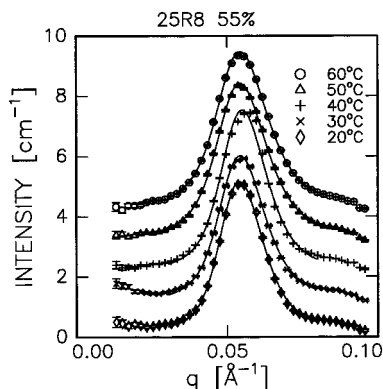


**Figure 3.** Representative scattering data of 55% 25R8 as measured at temperatures from 20 to 60 °C. The solid line represents a least-squares fit using the Percus–Yevick hard-sphere model. The 30, 40, 50, and 60 °C spectra have been shifted by respectively 1, 2, 3, and 4  $\text{cm}^{-1}$ .

In contradiction to these parameters characterizing the micellar size, the apparent micellar volume fraction,  $\phi$ , shows a sharp 10% change in magnitude at the sol–gel transition temperature of  $T_c = 42$  °C (Figure 2c). On both sides of  $T_c$ , the micellar density is basically constant, equal  $\phi = 0.47$  and  $\phi = 0.43$  below and above  $T_c = 42$  °C, respectively.

The micellar parameters in the liquid phase are consistent with expectations assuming that all polymers are associated in the network of spherical micelles with cores of basically pure propylene oxide. From the chemical formula, we have that 20% of the dry polymer is PPO, which in the 55% solution gives a PPO concentration  $c_{\text{PPO}} = 11\%$ . From the scattering function, we find correspondingly that  $\phi_{\text{core}} = (R_c/R_{\text{hs}})^3\phi = 0.11$  in the liquid phase.

The apparent change in micellar volume fraction is probably not reflecting a true change in the number of micelles. Rather, the change in  $\phi$  value reflects the weak first-order order-to-disorder transition, with pseudo-long-range correlations within ordered domains. (In the ordered phase, the structure factor of liquids is strictly not valid.)

While the 25R8 suspensions at high temperatures (55% above 42 °C) show azimuthally isotropic scattering patterns, marked texture appears when measured at temperatures below  $T_c = 42$  °C, as shown in Figure 4a and Figure 4b, respectively. This texture formation is reproducible within approximately 1 °C. The intense spots on the Debye–Scherrer ring in Figure 4b are significantly more narrow than the underlying ring of scattering, indicating coexistence of crystalline and liquid phases. This is in agreement with the resulting volume fraction of  $\phi = 0.47$ , which is the lower value expected for coexisting crystalline and liquid domains of suspensions of spherical colloids.<sup>12</sup> It is accordingly reasonable to conclude that the solid phase of the spherical PEO–PPO–PEO micelles constitute an ordered cubic structure.

While the order-to-disorder transition in PEO–PPO–PEO micellar suspensions can be understood as a simple hard-sphere crystallization resulting from an *increasing density of micelles*,<sup>6</sup> we do not see a similar origin for the  $T = 42$  °C transition in 25R8. One may speculate whether the melting of the cubic mesophase at  $T_c = 42$  °C should be treated as thermally driven in analogy with melting of classical crystals or whether it is more like the order-to-disorder transition in block copolymer melts driven by the Flory–Huggins interaction parameter

between the different blocks; for the latter case, the present system should be treated as a triblock copolymer “melt” of PPO and hydrated PEO, basically without any free water.

It may be noted that the intense Bragg peaks of the quenched sample shown in Figure 4b tend to lie on two concentric circles, whose radii have the ratio 1.15. This value is exactly the ratio between the first two reflections in the face-centered cubic (FCC) structure, (111) and (200), with ratio  $(4/3)^{1/2}$ , suggesting that phase II has FCC symmetry. For a perfect powder, the Bragg scattering gives Debye–Scherrer rings with nominal  $q$  values, which can be analyzed simply. In the case of small-angle neutron scattering of textured samples, however, the poor instrumental resolution makes the distribution of Bragg peaks less clear. Large crystallites which do not fulfill the Bragg condition with the nominal wavevector of the neutron beam may therefore still give rise to relative intense reflections on the two-dimensional detector, but with a  $q$  value which is slightly off the expected value. Even though the scattering pattern points to a face-centered structure, higher order reflections beyond the tight (111) and (200) are absent, making an unambiguous verification of the FCC symmetry impossible. In view of the PEO–PPO–PEO type of micelles forming a body-centered cubic structure (BCC), it seems rather surprising that 25R8, which has a large PEO content, should form a FCC structure. It should be noted, however, that in the 55% suspension, all the water is presumably tightly bound to the PEO backbone, making the system rather different from that of traditional Pluronics where the cubic phase typically appears within the 20–30% polymer regime.

Under steady shear (shear rate  $\dot{\gamma} \sim 1\text{--}10\text{ s}^{-1}$ ), the scattering pattern of phase II transforms into a pattern of six spots (Bragg peaks), as shown in Figure 4c, proving that the suspension has formed an ordered phase, presumably with cubic symmetry. No high-order reflections are visible. The six-spot pattern already appears after a few minutes (or less) of shear and remains unchanged for hours. The six reflections remain unchanged when the shear is stopped. In the  $xz$  scattering plane shown in Figure 4c ( $x$  being horizontal on the figure, and  $z$  vertical), we use the standard notation for the  $x$ ,  $y$ , and  $z$  axes being parallel to respectively shear flow, shear gradient, and neutral (another commonly used notation is  $v$ ,  $\nabla$ , and  $e$  for respectively  $x$ ,  $y$ , and  $z$ ).

The six Bragg reflections observed on the two-dimensional detector are not distributed with 60° intervals. Four of the observed peaks are separated by angles of 52° and two (around the horizontal flow axis) by angles of 76°. This deviation from perfect threefold symmetry in 25R8 may be a result of elastic deformation of the network when exposed to shear, or—more likely—it may be a result of nonperfect structure due to crystal planes that slip past one another in the sheared suspension, as observed in related colloidal systems.<sup>13,14</sup> The scattering pattern is actually very similar to the data observed in a FCC lattice of block copolymer micelles of polystyrene–polyisoprene,<sup>14</sup> which was analyzed according to a model of Ackerson and Loose, who described such colloidal structures as a zigzag path between two possible FCC registration paths.<sup>13</sup> The rather poor resolution and absence of higher order reflections in our scattering data prevent unfortunately detailed analysis in terms of such a model.

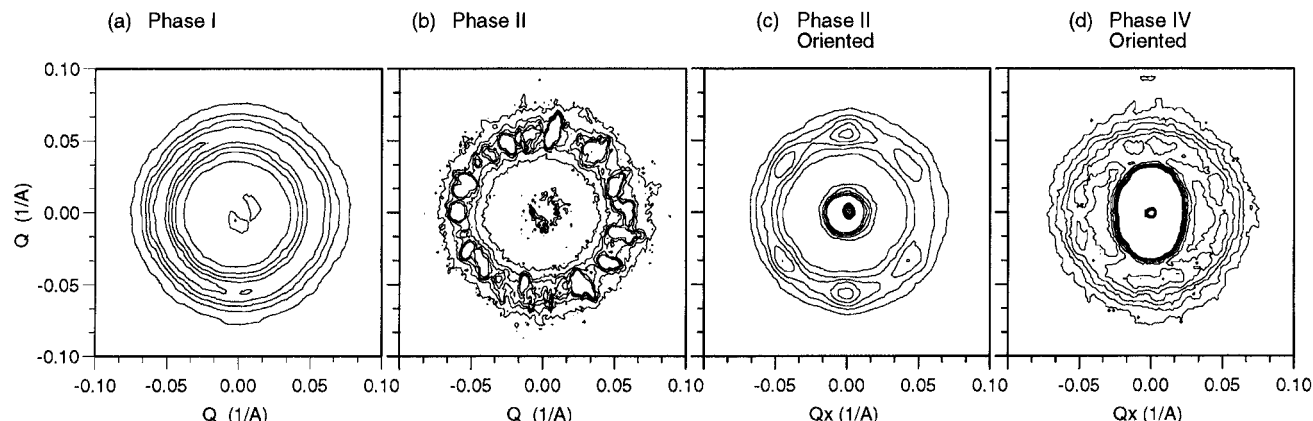


**Figure 4.** Two-dimensional scattering patterns of a 55% 25R8 suspension obtained in (a) the liquid phase I (55% polymer at 43 °C); (b) the solid cubic phase II (55% polymer at 41 °C) when quenched from phase I and (c) when shear-aligned; and (d) the solid phase IV which constitutes a mixture of crystalline PEO in the lamellar structure and amorphous micelles.

While PEO–PPO–PEO type micelles in shear have been proven to form a monodomain BCC phase with [111] planes perpendicular to the shear gradient,<sup>4,6</sup> it thus appears that the cubic phase(s) of 25R8 give a different structure. This could result from the reversed polymer architecture or may be due to a higher polymer concentration. Colloidal and micellar systems commonly form twinned structures of either BCC or FCC, when exposed to shear.<sup>13–15</sup>

While the pattern shown in Figure 4c is qualitatively similar to those obtained in various other systems of cubic colloids and micelles,<sup>6,13,14</sup> we have also obtained from 25R8 a pattern rotated 90° relative to the one shown, indicating that the energy difference between these two orientations in the shear field is small. In the PEO–PPO–PEO type of micellar phases, similar phenomena were observed only in the vicinity near  $T_c$ , where crystalline and liquid domains coexist due to the first-order nature of the order-to-disorder transition ( $0.47 < \phi < 0.53$  range). The two possible orientations of the cubic 25R8 phase may equivalently be related to inhomogeneity in the micellar network. This is in agreement with the relatively low value of  $\phi = 0.47$ , as discussed above and the lack of higher order reflections of the ordered phase. Furthermore, we find that in more dilute phases, large domains of micellar networks appear in excess water,<sup>9</sup> and it is likely that inhomogeneity in the connectivity density remains in the concentrated solutions. Additional evidence for irregularities in the PPO–PEO–PPO micellar network may be taken from studies of related systems of micellar networks, e.g., micelles of triblock copolymer of polystyrene end blocks with a middle block of poly(ethylene-propylene) dissolved in oil. These materials give a butterfly-shaped scattering pattern when stretched, revealing major inhomogeneity.<sup>16,17</sup>

When passing the low-temperature transition temperature, as observed rheologically, at  $T_s = 30$  °C, there is, within experimental statistics, no observable change in the scattering function in the measured  $q$  range and thus no change in the resulting  $R_c$ ,  $R_{hs}$ , and  $\phi$  parameters.

If the sample was quenched into phase III from the high-temperature disordered phase, we were not able to shear align it into a well-defined mono- or twin-domain structure. Rather, we typically observed a pseudosquare symmetry with azimuthally broad peaks both along the  $x$  axis parallel to shear flow and along the neutral  $z$  axes. The scattering pattern probably reflects that domains of the two orientations observed

in phase II both exist in large amounts. On cooling through the sub-transition temperature  $T_s$  observed rheologically, we see no changes in scattering pattern even if the sample is shear aligned in phase II. The sixfold pattern then remains unchanged when cooled into phase III.

We can accordingly not draw concrete conclusions regarding the phase III structure or the origin of the very high elastic modulus. Since it appears that there is no observable change in the organization of the micelles, the II–III transition seems not to be a transition between different cubic phases, as BCC–FCC for example observed in other solids, or between more complex phases as observed in melts and solutions of related PEO block copolymers.<sup>18,19</sup> One may speculate that the transition is related to properties of the entangled PEO chains, or possibly a matter of single-chain dynamics related to details in the structured water near the PEO backbone. Other types of experiments are needed, however, to reveal the true nature of the II–III transition.

At higher polymer concentrations, the rheological observations indicate a transition which at first sight seems similar to that discussed above. However, in contradiction to the characteristics of crossing the II–III transition, marked changes appear in the scattering function simultaneously with the changes in elastic moduli crossing the transition from phase II (or from phase I) to phase IV, thus proving that phases III and IV are not the same. In phase IV additional small-angle scattering appears, which we attribute to formation of a two-phase system:<sup>9</sup> one phase is dominated by the micellar structure; the other phase is a slightly swollen version of the lamellar phase observed in bulk PPO–PEO–PPO (and other PEO related) block copolymers where the PEO blocks are ordered in crystalline lamellae.<sup>9,18</sup> When exposed to shear the lamellar phase orients partly as demonstrated in the scattering pattern shown in Figure 4d and discussed previously.<sup>9</sup>

#### IV. Conclusion

We have shown that it is possible to form a mono (or twin) domain cubic phase of interconnected micelles. This is observed in aqueous systems of PPO–PEO–PPO triblock copolymers. The ability for PPO–PEO–PPO-based micelles to transform into a well-defined domain structure is probably sensitively related to the possibility for the end blocks to move from one micelle to another. Similar effects cannot be expected in micellar

networks of for example PS-PEP-PS, where the micellar cores are PS in the glassy state.

The low-temperature solid phase III still seems to be cubic ordered spherical micelles. It is speculated that the additional modulus is a matter of single-chain dynamics, possibly related to details in the structured water near the PEO backbone. The additional modulus in phase IV is also related to dynamics of the PEO chain, which becomes crystalline layered.

## References and Notes

- (1) Chu, B. *Langmuir* **1995**, *11*, 414.
- (2) Almgren, M.; Brown, B.; Hvidt, S. *Colloid Polym. Sci.* **1995**, *273*, 2.
- (3) Alexandris, P.; Athanassiou, V.; Hatton, T. A. *Langmuir* **1995**, *11*, 2442.
- (4) Mortensen, K. *J. Phys. Condensed Matter* **1996**, *8*, A103.
- (5) Wanka, G.; Hoffmann, H.; Ulbricht, W. *Colloid Polym. Sci.* **1990**, *268*, 101.
- (6) Mortensen, K.; Brown, W.; Nordén, B. *Phys. Rev. Lett.* **1992**, *13*, 2340.
- (7) Mortensen, K. *Europhys. Lett.* **1992**, *19*, 599.
- (8) Mortensen, K.; Pedersen, J. S. *Macromolecules* **1993**, *26*, 805.
- (9) Mortensen, K.; Brown, W.; Jørgensen, E. *Macromolecules* **1994**, *27*, 5654.
- (10) Mortensen, K.; Almdal, K.; Bates, F. S.; Koppi, K.; Tirrell, M.; Nordén, B. *Physica B* **1995**, *213*, 682.
- (11) See, for example: Kinning, D. J.; Thomas, E. L. *Macromolecules* **1984**, *17*, 1712.
- (12) Pusey, P. N.; van Megen, W. *Nature* **1986**, *320*, 340.
- (13) Loose, W.; Ackerson, B. J. *J. Chem. Phys.* **1994**, *101*, 7211.
- (14) McConnell, G. A.; Lin, M. Y.; Gast, A. *Macromolecules* **1995**, *28*, 6754.
- (15) Almdal, K.; Koppi, K. A.; Bates, F. S. *Macromolecules* **1993**, *26*, 4058.
- (16) Reynders, K.; Mischenko, N.; Mortensen, K.; Overbergh, N.; Reynaers, H. *Macromolecules* **1995**, *28*, 8699.
- (17) Mischenko, N.; Reynders, K.; Mortensen, K.; Reynaers, H. *J. Polym. Sci., Polym. Phys. Ed.* **1996**, in press.
- (18) Hillmyer, M.; Bates, F. S.; Almdal, K.; Mortensen, K.; Ryan, A. *Science* **1996**, *271*, 976.
- (19) Hillmyer, M.; Bates, F. S.; Almdal, K.; Mortensen, K., to be published.

MA960457M